

# Plasma Sprayed AlCoCrFeNi and MnCoCrFeNi High Entropy Alloys: High Temperature Stability, Coating Elastic Properties and Surface Roughness

Andrew S.M. Ang<sup>1</sup>, Christopher C. Berndt<sup>2</sup>, Mitchell L. Sesso<sup>3</sup>,  
Ameey Anupam<sup>4</sup>, S. Praveen<sup>5</sup>, Ravi Sankar Kottada<sup>6</sup> and B.S. Murty<sup>7</sup>

<sup>1,2,3</sup>Industrial Research Institute Swinburne, Swinburne University of Technology,  
H66, P.O. Box 218, Hawthorn, Victoria 3122, Australia

<sup>2</sup>Adjunct Professor, Department of Materials Science and Engineering,  
Stony Brook University, Stony Brook, NY11794, USA

<sup>4,5,6,7</sup>Department of Metallurgical and Materials Engineering,  
Indian Institute of Technology Madras, Chennai-600036, India

E-mail: <sup>2</sup>cberndt@swin.edu.au

**Abstract**—High Entropy Alloys (HEAs) are a new class of alloys with multi-principle elements mixed in equi-atomic ratio resulting in simple solid solutions. HEAs are known for their high temperature microstructural stability, and enhanced oxidation and wear resistance. Apart from bulk material processing routes such as casting and sintering, HEAs can also be deposited as a surface coating. In the present study, thermal sprayed HEA coatings are investigated as an alternative bond coat material for a thermal barrier coating system. Nano structured HEA powders of AlCoCrFeNi and MnCoCrFeNi were prepared by ball milling and then plasma sprayed. Subsequently, the high temperature stability of the HEA powders as well as the as-sprayed coating mechanical properties and coating surface roughness of both HEA coatings were characterized.

**Keywords:** High Entropy Alloys, High Temperature Stability, Hardness Properties, Surface Roughness Properties, Bond Coat, Thermal Spray

## INTRODUCTION

The thermal spray process is a technically-effective coating technology that can be applied to a wide range of industrial applications. Coating materials are heated to, or near to, their melting points. The molten or partially molten droplets are then accelerated in a gas stream and projected against the surface to be coated [1].

Among the various thermal spray techniques, atmospheric plasma spray (APS) has been successfully used since the 1980s in the manufacture of advanced zirconia-based thermal barrier coatings (TBCs) for gas and land turbines. TBCs are duplex coating systems typically consisting of a stabilized zirconia coating over a metal bond coating [2, 3] and allow engine operation above 1,000°C. In particular, traditional MCrAlY bond coats (with M= Ni, Co or their combination) are critical to the coating system's survivability because it acts as a protective layer between the porous ceramic top coat and the substrate during exposure to the high temperature oxidizing environment. Bond coats also accommodate differences in coefficient of thermal expansion (CTE) between ceramic topcoats and metallic substrates under the operational thermal cycle conditions.

With the developments in High Entropy Alloys (HEAs) [4], a new class of alloys with multi-principle elements in equi-atomic ratio, a suitable elemental composition could potentially be formulated for TBC bond coat applications. HEAs are known for their high temperature microstructural stability and enhanced oxidation resistant properties. The HEA class of materials have the tendency to form simple solid solution phases, such as FCC and BCC phases, rather than intermetallic

compounds. Hence HEA microstructures retain good thermal stability [4, 5]; which is an attribute for a TBC application.

The current studies have focused on nanostructured HEA powders of AlCoCrFeNi and MnCoCrFeNi prepared *via* mechanical alloying and, subsequently, deposited by the APS technique. Previous studies have shown that the microstructure of HEA feedstock was controlled by selection of the milling conditions for mechanical alloying; while the plasma spray parameters for coating deposition were optimised using an in-flight particle diagnostic tool and assessing splat microstructures. The coating microstructures were also characterised to understand the mechanical responses under load.

In this current contribution, the high temperature stability of the HEA powders as well as the as-sprayed coating elastic modulus and surface roughness were evaluated. Within the context of thermal spray coating development, these properties are important to evaluate the potential of HEAs as a TBC bond coat material.

## EXPERIMENTAL DETAILS

### High Entropy Alloy Plasma Spray Coatings

Elemental powders of Al, Co, Cr, Fe, Ni and Mn with purity greater than 99.5 % were used to synthesize AlCoCrFeNi and MnCoCrFeNi HEAs *via* the mechanical alloying route. The milling parameters were 300 rpm speed and a ball to powder weight ratio of 10:1. Coating samples were deposited using a conventional air plasma spray system (Metco 7MB, Sulzer Metco Inc., Westbury, NY-USA) that employed argon as the primary plasma

operating gas and hydrogen as the secondary gas to increase the overall plasma jet temperature. Details of the coating parameter conditions can be found in Table 1.

Table 1: Plasma Spray Operating Parameters

7MB Plasma spray operating parameter	
Current (A)	300
Voltage (V)	65
Primary gas flow, Ar (slpm)	42.1
Secondary gas flow, H <sub>2</sub> (slpm)	2.35
Powder feed rate (g/min)	17-21
Powder carrier gas flow, Ar (slpm)	6
Stand-off distance (mm)	90
Nozzle type	GH

### Powder Characterization

A Bruker X-ray diffractometer (XRD) with Cu-K $\alpha$  radiation at 40 kV and 30 mA was used to identify the phases present in the feedstocks and coatings. A 0.5° scanning step was employed with a 10 s dwell time. Peaks of the individual phases were identified and indexed by comparison of the diffraction pattern to a known standard from the International Centre for Diffraction Data's Powder Diffraction File (ICDD PDF).

### Coating Characterization

The cross section profiles of HEA coatings were prepared according to ASTM E1920: Standard Guide for Metallographic Preparation of Thermal Sprayed Coatings [6]. Grinding and polishing was performed to obtain a surface that was appropriate for characterisation by microscopy and indentation hardness tests. Knoop microhardness testing (Micromet 2103 Microhardness Tester, Buehler, USA) was performed on the cross sectioned coating samples to determine the mechanical response of the HEA coatings. The application time of the full test load was 15 s.

The Knoop method is a sensitive test with respect to the orientation of the lamellar microstructure of the coating [7]. Thus, the Knoop test provides information that is difficult to achieve from the conventional Vickers method.

The as-sprayed HEA coating roughness values were measured using a 3D-optical profiler system (WykoContour GT-K1, Bruker, USA). The scanner assembly operates on the principal of vertical scanning interferometry. The internal translator moves the objective while the camera periodically records frames. The "interference" used to calculate the surface height is achieved inside the measurement objective by splitting the light into reference and measurement beams. Multiple path images can be scanned and combined by the machine's software to form a 3D surface representation.

## RESULTS AND DISCUSSION

### Phase Evolution at Elevated Temperatures

The elemental powder blends were mechanically alloyed for 10 hours. The XRD patterns revealed contrasting phase differences, see Fig. 1. Mechanical alloyed HEA powders of AlCoCrFeNi form a major BCC phase with a minor FCC phase. On the contrary, MnCoCrFeNi powder yields a major FCC phase with a minor BCC phase.

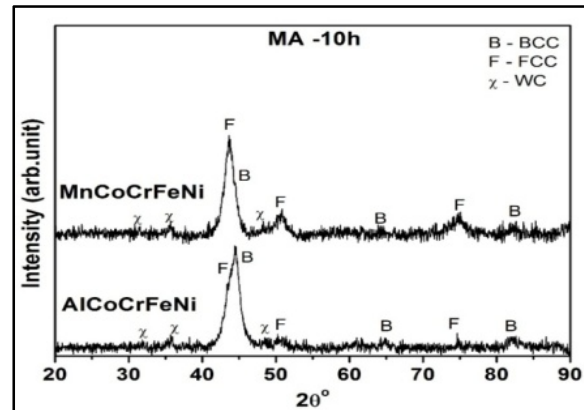


Fig. 1: XRD patterns of 10 h Milled AlCoCrFeNi and MnCoCrFeNi HEAs. Low Levels of Tungsten Carbide from the Milling Balls Can be Detected

However, after undergoing the high temperature plasma spray process, the XRD patterns of the AlCoCrFeNi and MnCoCrFeNi coatings revealed the FCC phase as the major phase with minor oxide peaks, see Figures 2 and 3.

While the plasma spray process exposes the HEAs to intermittent high temperatures, it is not analogous to conditions when a TBC bond coat is exposed to elevated temperatures in an oxidising environment. Under conventional operating conditions the high temperature isothermal oxidation promotes the formation of a thermally grown oxide (TGO) layer [8] that contributes to failure [9] of the TBC system. Therefore, to understand the possible high temperature phase transformation, the HEA powders were heat treated at 850°C for 3 hours under a normal atmosphere. The treatment assesses the isothermal oxidation resistance of HEAs and any formation of oxides or intermetallic phases would be subsequently detected in the XRD spectra, see Figures 2 and 3.

Comparisons between the plasma sprayed HEA coating and heat treated HEA powder provide insights into additional phase formations during a thermal cycling process [10]. Peaks corresponding to FCC phase were detected for AlCoCrFeNi after the heat-treatment process, see Figure 2. No oxide phases were detected. This result implies that this HEA composition has the tendency to (i) form stable FCC phase at high temperatures, and(ii)

exhibits isothermal oxidation resistant properties. It is also confirmed that the formation of oxides in AlCoCrFeNi plasma sprayed coatings occurs during the feedstock melting and re-solidification processes.

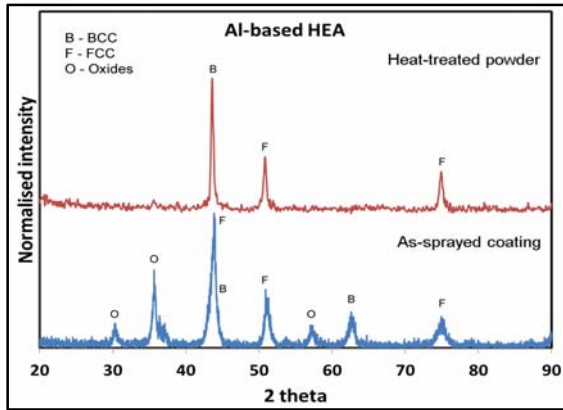


Fig. 2: XRD Patterns of AlCoCrFeNi Plasma Sprayed Coatings and Heat Treated Powder

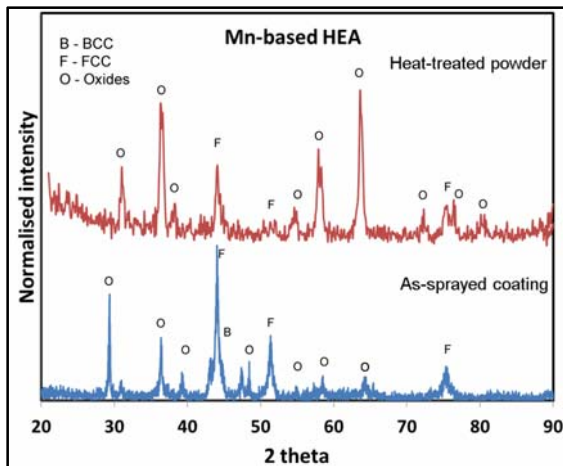


Fig. 3: XRD Patterns of MnCoCrFeNi Plasma Sprayed Coatings and Heat Treated Powder

Figure 2 indicates that the high temperature stable structure for AlCoCrFeNi is possibly FCC since the heat treated sample exhibited mostly a single FCC phase in comparison to the major BCC phase that was observed in the as-milled state (Figure 1). In addition, the plasma sprayed condition shows FCC peaks to be the most intense; thereby, indicating the stability of this phase.

From Figure 3, the MnCoCrFeNi XRD patterns revealed the formation of metal oxides during heat treatment. These oxides corresponded to a mixture of Fe<sub>3</sub>O<sub>4</sub>, some possible binary oxides of the form A<sub>2</sub>BO<sub>4</sub> (A, B = Co, Fe, Ni, Cr or Mn), and ternary oxides of the form ABCO<sub>4</sub> (A, B, C = Co, Fe, Ni, Cr or Mn). The intensity of the XRD peak can be interpreted as being related to the degree of oxidation. Thus, there was significantly less retained metallic HEA after heat

treatment since the intensity of FCC peaks is lower compared to those of oxide phases. There is an indication of poor (i) phase stability and (ii) oxidation resistance of MnCoCrFeNi at 850°C.

Although the MnCoCrFeNi feedstock had undergone exposure to an intermittent high temperature environment during the plasma spray process, the intensity of oxide peaks were lower in comparison to those of FCC phase, and in comparison to heat treated powders. Therefore, the growth of detrimental TGO is expected for MnCoCrFeNi bond coats compared to those of AlCoCrFeNi composition during a high temperature thermal cycling process.

### Indentation Response and Coating Modulus

The anisotropic mechanical behaviour of the coating cross sectional microstructure was determined by Knoop microhardness tests where the indenter minor axis was oriented in two directions: (i) along the lamellar layers, and (ii) against (or perpendicular to) the lamellar layers. These results are shown in Table 2 and Table 3.

Table 2: Knoop Hardness of APS AlCoCrFeNi Coating

Orientation		300 g		Can Compare Dataset?
		d1 (µm)	HK (GPa)	
Along lamellar layers (n = 15)	Average	105	3.86	Yes P value= 4.43E-06
	Standard Deviation	8.48	0.57	
	COV	8%		
Against lamellar layers (n = 15)	Average	92.8	4.87	
	Standard Deviation	2.87	0.31	
	COV	3%		

Table 3: Knoop Hardness of APS MnCoCrFeNi Coating

Orientation		300 g		Can Compare Dataset?
		d1 (µm)	HK (GPa)	
Along lamellar layers (n = 15)	Average	102	4.09	Yes P value= 4.72E-02
	Standard Deviation	6.95	0.47	
	COV	7%		
Against lamellar layers (n = 17)	Average	97.7	4.51	
	Standard Deviation	10.4	0.77	
	COV	11%		

Statistical t-testing at 95% significance showed that that the data sets arose from different populations. It was, therefore, possible to quantify that the mechanical strength perpendicular to lamellae was higher than parallel to the lamellar layers.

The Knoop indentation method as described by Marshall *et al.* [11] was adopted to measure the coating elastic modulus. During the indentation process, an elastic-plastic field develops and the deformed coating is comprised of elastic and inelastic behaviour. In the fully loaded state, the ratio of the diagonal dimensions, *a* (major) and *b* (minor) of the Knoop contact area can be

defined by the indenter geometry,  $a/b = 7.11$ . Elastic recovery during the unloading cycle reduces the length of the diagonals and indentation depth. The reduction in length will be evident for the minor diagonal,  $b'$ , while the major diagonal change,  $a'$ , is negligible. Therefore, the mathematical relationship of the displacement can be summarised as follows:

$$\frac{b'}{a'} \approx \frac{b'}{a} = \frac{b}{a} - \frac{\alpha H}{E}$$

Rearranging for elastic modulus,  $E$ , derived:

$$E = \frac{\alpha a H}{b - b'}$$

where,  $H$  is the Knoop hardness (in  $GPa$ ),  $\alpha$  is a constant determined by Marshall [11] to be 0.45. More details on the test can be found in reference [7].

Importantly, the measurement depends on the elastic recovery of the minor diagonal,  $b'$ , and therefore its alignment is sensitive to the coating's anisotropic microstructure. In this study, the minor diagonal,  $b'$ , for both AlCoCrFeNi and MnCoCrFeNi were aligned along the lamellar layers, see Figure 4. For AlCoCrFeNi APS coatings the elastic modulus is  $161 \pm 46$  GPa ( $n=10$ ) while the MnCoCrFeNi coatings exhibited a lower elastic modulus of  $129 \pm 31$  GPa ( $n=10$ ), where "n" is the number of images considered in the analysis. The elastic modulus values obtained in the current study are comparable to those of conventional bond coat NiCrAlY material,  $E_{NiCrAlY} \sim 190$  GPa [12], with similar porosity levels.

A lamellar microstructure, typical of thermal spray coatings, was observed in both HEA plasma spray coatings, as illustrated in Figure 4. This layered structure is littered with numerous voids that can be classified as pores, as well as interlamellar cracks that also contribute to the porosity. The measured porosity levels for AlCoCrFeNi and MnCoCrFeNi coatings, determined by image analysis, are  $9.5 \pm 2.3\%$  ( $n = 7$ ) and  $7.4 \pm 1.3\%$  ( $n = 9$ ), respectively.

### Surface Roughness Profile of HEA Coatings

The as-sprayed surface roughness profile is a function of the plasma spray parameters, torch movement profile and feedstock characteristics. The achieved as-sprayed roughness profile is critical for bond coats because it forms the underlying surface onto which the ceramic top coat is deposited.

The use of an instrumented optical profiler has advantages over the traditional contact stylus probe. For instance, the  $5 \mu m$  diameter of the stylus tip places a limitation on the size of surface features that may be measured. The stylus also translates only along a single axis, hence requiring a large sample size to obtain a representation of the surface profile. There are other

inadequacies relating to 2D "R" parameters versus use of 3D "S" parameters [13].

As shown in Table 4, the surface profile of the as-sprayed coating is typical to those obtain by conventional plasma sprayed bond coats. The distribution of skewness,  $S_{sk}$ , was close to zero and implied that there was an approximately equal amount of surface valleys and peaks. The kurtosis,  $S_{klt}$ , readings, which were approximately equal to 3, agreed with this interpretation and indicated that the distribution of spikes and depressions were random.

Figures 5 and 6 show the 3D representation of the surface profile of the plasma sprayed coatings. The outline of the flattened splats can be identified from these plots. The splats can be characterized as possessing a well-flattened morphology.

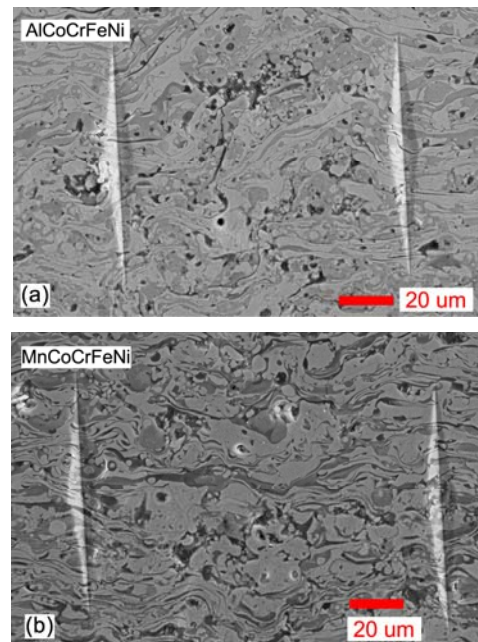


Fig. 4: SEM Micrographs of (a) AlCoCrFeNi and (b) MnCoCrFeNi HEA Coating with Knoop Imprints

*Note:* The Knoop indenter in these images is defined as being aligned "along" lamellae.

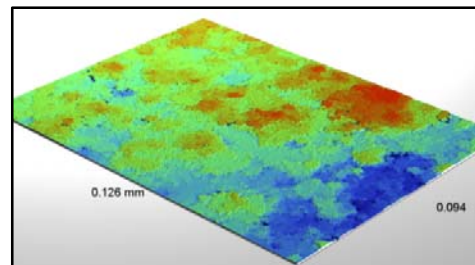


Fig. 5: 3D Reconstruction of Surface Profile of Plasma Sprayed AlCoCrFeNi Coatings

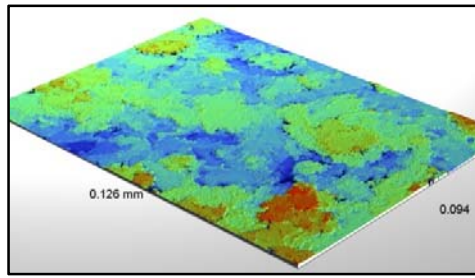


Fig. 6: 3D Reconstruction of Surface Profile of Plasma Sprayed MnCoCrFeNi Coatings

## CONCLUSION

The following conclusions can be interpreted within the context of this current work:

1. Nanostructured HEA AlCoCrFeNi and MnCoCrFeNi powders were prepared by mechanical alloying equi-atomic proportions of the constituent elements. The major phase formed after mechanical alloying for AlCoCrFeNi powders was BCC. In contrast, FCC phase was dominant for the MnCoCrFeNi powders.
2. The lamellar plasma sprayed microstructure of both HEA coatings exhibited a majority of FCC phases. Minor oxide phases formed due to the high temperature coating process.
3. The high temperature heat treatment of the HEA powders indicated that FCC phase forms without

oxides for the AlCoCrFeNi composition. This transformation behavior is expected to be beneficial within a high temperature thermal cycling environment.

4. An anisotropic mechanical response of the HEA coatings was determined by performing Knoop microhardness measurements. The elastic modulus of the AlCoCrFeNi APS coatings was 161 GPa while the MnCoCrFeNi coatings showed a lower elastic modulus of 129 GPa. These values are comparable to conventional MCrAlY plasma sprayed bond coats.
5. The as-sprayed roughness profile is between  $S_a = 7.88$  for AlCoCrFeNi APS coatings and  $S_a = 9.93$  for the MnCoCrFeNi coatings. These roughness values are comparable to those of conventional plasma sprayed bond coats.

## ACKNOWLEDGEMENT

The authors acknowledge the technical assistance and contributions of Mr Andrew Moore. This research was initiated under a cooperative agreement between Swinburne University of Technology (SUT) and the Indian Institute of Technology–Madras (IIT-M). The authors are grateful to the President and Director of these institutions, respectfully, that has allowed this research to evolve.

CCB acknowledges the support of an ASM/IIM Award that has enabled this work to be presented in India.

Table 4: Summary of “S” Surface Roughness Parameters for AlCoCrFeNi and MnCoCrFeNi APS Coatings

	Average Roughness $S_a$ ( $\mu\text{m}$ )	Root Mean Square Roughness $S_q$ ( $\mu\text{m}$ )	Max. Height of Surface $S_z$ ( $\mu\text{m}$ )	Max. Peak Height $S_p$ ( $\mu\text{m}$ )	Max. Valley Depth $S_v$ ( $\mu\text{m}$ )	Skewness $S_{sk}$	Kurtosis $S_{ku}$
AlCoCrFeNi	7.88	10.43	109.58	71.10	-38.48	0.67	5.66
MnCoCrFeNi	9.93	12.67	101.25	48.98	-52.27	0.40	3.30

## REFERENCES

- [1] Davis, J.R. (2004), *Handbook of Thermal Spray Technology*, Materials Park, OH, USA: ASM International.
- [2] Stecura, S. (1976), “Two-layer Thermal Barrier Coating for Turbine Airfoils-furnace and Burner Rig Test Results”, Lewis Research Center, National Aeronautics and Space Administration: Cleveland, Ohio 44135.
- [3] Stecura, S. (1977), *Thermal Barrier Coating System*, U.S. Patent Office, Editor, The United States of America as Represented by the Administrator of the National Aeronautics and Space Administration: United States.
- [4] Yeh, J.W. *et al.* (2004), “Nanostructured High-entropy Alloys with Multiple Principal Elements: Novel alloy Design Concepts and Outcomes”, *Advanced Engineering Materials*, Vol. 6(5), pp. 299–303+274.
- [5] Tong, C.J., *et al.* (2005), “Microstructure Characterization of AlxCoCrCuFeNi High-entropy Alloy System with Multiprincipal Elements”, *Metallurgical and Materials Transactions A: Physical Metallurgy and Materials Science*, Vol. 36(4), pp. 881–893.
- [6] ASTM E1920-03(2008), “Standard Guide for Metallographic Preparation of Thermal Sprayed Coatings”, 2008, ASTM International: West Conshohocken, PA.
- [7] Ang, A.S.M. and Berndt, C.C. (2014), “A Review of Testing Methods for Thermal Spray Coatings”, *International Materials Reviews*, 59(4), pp. 179–223.
- [8] Choi, H., *et al.* (2002), “Isothermal Oxidation of Air Plasma Spray NiCrAlY Bond Coatings”, *Surface and Coatings Technology*, Vol. 150(2–3), pp. 297–308.
- [9] Darolia, R. (2013), “Thermal Barrier Coatings Technology: Critical Review, Progress Update, Remaining Challenges and Prospects”, *International Materials Reviews*, Vol. 58(6), p. 315–348.
- [10] Berndt, C.C. and Miller, R.A. (1984), “Failure Analysis of Plasma-Sprayed Thermal Barrier Coatings”, *Thin Solid Films*, Vol. 119(2), pp. 173–184.
- [11] Marshall, D.B., Noma, T. and Evans, A.G. (1982), “A Simple Method for Determining Elastic-Modulus-to-Hardness Ratios using Knoop Indentation Measurements”, *Journal of the American Ceramic Society*, Vol. 65(10), pp. 175–176.
- [12] Rico, A., *et al.* (2009), “Mechanical Properties of Thermal Barrier Coatings after Isothermal Oxidation”, *Depth Sensing Indentation Analysis Surface and Coatings Technology*, Vol. 203(16), pp. 2307–2314.
- [13] Ang, A.S.M. (2013), *Mechanical Properties of Ceramic Thermal Sprayed Coatings*, Ph.D Thesis, Faculty of Engineering and Industrial Sciences, Swinburne University of Technology.